
Article:
Semenova, Olga, Richardson, Peter Michael orcid.org/0000-0002-6631-2459, Parrott, Andrew et al. (3 more authors) (2019) Reaction monitoring using SABRE-hyperpolarized benchtop (1 T) NMR spectroscopy. Analytical Chemistry. 9b00729. pp. 6695-6701. ISSN 0003-2700

https://doi.org/10.1021/acs.analchem.9b00729

---

analytical chemistry

Article

Cite This: Anal. Chem. XXXX, XXX, XXX−XXX

pubs.acs.org/ac

Reaction Monitoring Using SABRE-Hyperpolarized Benchtop (1 T) NMR Spectroscopy

Olga Semenova,[†] Peter M. Richardson,[†] Andrew J. Parrott,[‡] Alison Nordon,[‡] Meghan E. Halse,*[,†] and Simon B. Duckett*[,†]

[†]Centre for Hyperpolarisation in Magnetic Resonance, Chemistry, The University of York, York YO10 5NY, U.K.

[‡]WestCHEM, Department of Pure and Applied Chemistry and CPACT, University of Strathclyde, Glasgow G11XQ, U.K.

Supporting Information

ABSTRACT: The conversion of [IrCl(COD)(IMes)] (COD = *cis*,*cis*-1,5-cyclooctadiene, IMes = 1,3-bis(2,4,6-trimethyl-phenyl)imidazole-2-ylidene) in the presence of an excess of *para*-hydrogen (p-H_2) and a substrate (4-aminopyridine (**4-AP**) or 4-methylpyridine (**4-MP**)) into $[Ir(H)_2(IMes)(substrate)_3]Cl$ is monitored by ^1H NMR spectroscopy using a benchtop (1 T) spectrometer in conjunction with the p-H_2-based hyperpolarization technique signal amplification by reversible exchange (SABRE). A series of single-shot ^1H NMR measurements are used to monitor the chemical changes that take place in solution through the lifetime of the hyperpolarized response. Non-hyperpolarized high-field ^1H NMR control measurements were also undertaken to confirm that the observed time-dependent changes relate directly to the underlying chemical evolution. The formation of $[Ir(H)_2(IMes)(substrate)_3]Cl$ is further linked to the hydrogen isotope exchange (HIE) reaction, which leads to the incorporation of deuterium into the *ortho* positions of **4-AP**, where the source of deuterium is the solvent, methanol-d_4. Comparable reaction monitoring results are achieved at both high-field (9.4 T) and low-field (1 T). It is notable that the low sensitivity of the benchtop (1 T) NMR enables the use of *protio* solvents, which when used here allows the effects of catalyst formation and substrate deuteration to be separated. Collectively, these methods illustrate how low-cost low-field NMR measurements provide unique insight into a complex catalytic process through a combination of hyperpolarization and relaxation data.

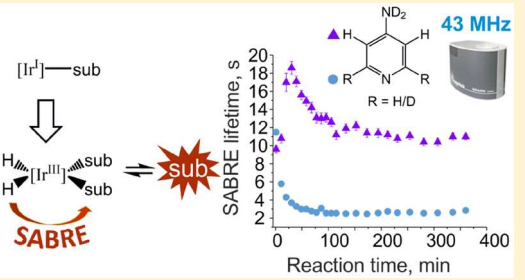

Reaction monitoring using process analytical technology (PAT) is an important part of synthetic optimization, reaction scale-up, and industrial quality control.[1] Although NMR spectroscopy is a well-established method for reaction monitoring, standard high-field (7−23 T) NMR spectrometers are large and costly to both purchase and operate, thereby making them poorly suited to PAT applications. Recently, low-cost benchtop NMR spectrometers, based on permanent magnets with field strengths around 1−2 T, have become available.[2] These offer an opportunity to address the issue of cost while also providing a level of detector portability.[2] However, these instruments suffer from relatively low sensitivity and reduced chemical shift dispersion due to the lower magnetic field strengths, which limits their viability for the study of low-concentration analytes and nuclei with low NMR receptivity such as ^{13}C. One potential solution to this issue is to combine benchtop NMR with hyperpolarization.

Hyperpolarization is a term used to describe methods that generate NMR signal responses that are enhanced relative to those associated with nuclear spins at thermal equilibrium in the detection field.[3] Some of the most popular hyperpolarization methods today are dynamic nuclear polarization (DNP),[4] spin-exchange optical pumping (SEOP),[5] and *para*-hydrogen induced polarization (PHIP).[6] In the context of industrial process monitoring, it is essential that the hyperpolarization process itself is low-cost and compact so that it does not compromise the advantages of benchtop NMR. Dissolution DNP has been integrated with benchtop NMR for monitoring the conversion of [1-^{13}C] pyruvate to [1-^{13}C] lactate *in vitro* and *in vivo*.[7] However, the generation of hyperpolarized compounds by dissolution DNP is time-consuming (ca. 90 min per hyperpolarized sample) as well as costly and requires equipment with a large footprint. In contrast, we focus here on PHIP methods, which are relatively inexpensive and yield hyperpolarization in seconds.[8]

In the traditional approach of Bowers and Weitekamp, *para*-hydrogen induced polarization (PHIP) is achieved through hydrogenation of the molecule under investigation.[8a,9] Introduced in 2009, the signal amplification by reversible exchange (SABRE) method is a non-hydrogenative version of PHIP that catalytically transfers p-H_2-derived polarization without changing the chemical structure of the target compound.[10] In this technique, p-H_2 and the target compound, often called the substrate, bind reversibly to the metal center of the SABRE catalyst (Figure 1). Once attached to the metal center, the magnetic symmetry of p-H_2 is broken, and the

Received: February 8, 2019
Accepted: April 15, 2019
Published: April 15, 2019

DOI: 10.1021/acs.analchem.9b00729
Anal. Chem. XXXX, XXX, XXX−XXX

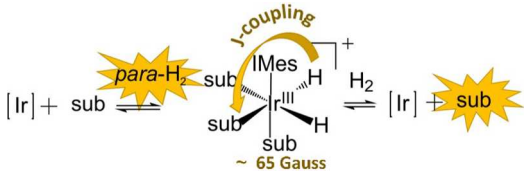

Figure 1. In the presence of an excess of *para*-hydrogen (p-H_2) and substrate, the exchange processes allows polarization transfer from p-H_2 such that NMR resonances of the free substrate are enhanced. This transfer occurs most often at a low magnetic field (0−200 G) through the scalar coupling network in the active complex and, because of its reversibility, operates continuously when fresh p-H_2 is supplied.

resultant hydride ligands are able to transfer their latent polarization into the bound substrate via the J-coupling network of the complex. This process can be optimized by using a weak magnetic field that often lies in the range of 0−200 G depending on the type of nucleus that is to receive the polarization.[11] The SABRE method is reversible, taking seconds to build up polarization, while target molecules can be repolarized by adding fresh p-H_2. Therefore, it provides a fast and renewable or indeed continuous route to hyperpolarization. As a result of the relatively cheap methods for generating and storing p-H_2 and the comparative simplicity of the SABRE method, this is an attractive approach for industrial process monitoring using hyperpolarized benchtop NMR.[8] Indeed, SABRE has already been combined with benchtop NMR to enhance ^{1}H, ^{13}C, and ^{15}N NMR signals.[12] One of the limitations of the SABRE method compared to other approaches such as DNP is the range of substrates that are amenable to hyperpolarization, with the best results being observed for N-heterocycles. However, many groups are working to expand the scope of the SABRE method in order to make it more generally applicable.[12d,13] Additionally a number of articles have proposed routes to achieve biocompatible SABRE hyperpolarization with a view to *in vivo* detection of biomolecules.[14]

In this work, we introduce a method to follow reactivity using single-shot measurements that probe both the lifetime and the magnitude of a SABRE-enhanced ^{1}H NMR response. Such measurements can be easily completed at either high or low field. To illustrate this method and its benefits, we follow the reaction in which the SABRE precatalyst converts into the active catalyst. Specifically, we monitor the formation of $[Ir(H)_2(IMes)(substrate)_3]Cl$ (IMes = 1,3-bis(2,4,6-trimethylphenyl)imidazole-2-ylidene).[15] Because iridium complexes facilitate the hydrogen isotope exchange (HIE) reaction, deuteration of the substrate is observed during this process in methanol-d_4.[10,16] High-field (9.4 T, 400 MHz) ^{1}H NMR detection is initially used to measure the changes in SABRE hyperpolarization lifetimes during the catalyst activation and HIE reactions. Parallel non-hyperpolarized ^{1}H NMR measurements are completed to link the observed changes in hyperpolarization lifetime to the underlying chemical changes in solution. Because of the reduced sensitivity and increased peak overlap in ^{1}H NMR spectra acquired at 1 T (43 MHz), standard ^{1}H NMR reaction monitoring of these processes cannot be achieved using benchtop NMR. We overcome these limitations by using our hyperpolarized response while also exploiting the inherent low sensitivity of a benchtop NMR spectrometer to allow experiments in nondeuterated solvents to fully differentiate the effects of the active SABRE catalyst formation from those of target substrate deuteration.

EXPERIMENTAL SECTION

Sample Preparation. NMR samples were prepared from a 0.6 mL solution of 5 mM [IrCl(COD)(IMes)] (COD = *cis,cis*-1,5-cyclooctadiene, IMes = 1,3-bis(2,4,6-trimethyl-phenyl)-imidazole-2-ylidene) in methanol-d_4 or *protio* methanol by adding 15 μmol of **4-AP** or **4-MP** (5 equivalents with respect to the SABRE precatalyst **1**) in a 5 mm NMR tube fitted with a Young's tap (GPE Scientific Ltd., Leighton Buzzard, UK). The samples were degassed using a three-stage freeze−pump−thaw method in a bath of dry ice and acetone. The precatalyst was synthesized in-house, and the **4-AP** and **4-MP** were purchased from Sigma-Aldrich (Sigma-Aldrich Company Ltd., Gillingham, UK) and used without further modification. ^{1}H, ^{13}C, and ^{15}N NMR characterization data for **4-AP**, **4-MP**, [Ir(COD)-(IMes)(substrate)]Cl, and $[Ir(H)_2(IMes)(substrate)_3]Cl$ (substrate = **4-AP** or **4-MP**) is available in the Supporting Information.

SABRE Catalyst Activation Monitoring Using Standard ^{1}H NMR. Solutions containing the precatalyst **1** with either **4-AP** or **4-MP** in methanol-d_4 or *protio* methanol formed the unactivated catalyst [Ir(COD)(IMes)(substrate)]-Cl. A 0.6 mL aliquot of this initial solution was added to a 5 mm NMR tube equipped with a Young's tap and degassed following the sample preparation procedure described above. When **4-MP** was used as the substrate, peaks corresponding to the precatalyst **1** were observed in the prepared solution and were quantified by ^{1}H NMR at 400 MHz as contributing 15% of the signal, suggesting 85% of **1** had converted to the unactivated catalyst [Ir(COD)(IMes)(**4-MP**)]Cl at equilibrium. In contrast, no ^{1}H NMR peaks corresponding to **1** were observed in the initial ^{1}H NMR spectra for samples where **4-AP** was used as the substrate, suggesting full conversion to **2**. When the conversion of precatalyst **1** into [Ir(COD)(IMes)-(**4-AP**)]Cl **2** was monitored by ^{1}H NMR spectroscopy for a sample containing 5 mM of **1** and 25 mM of **4-AP** in methanol-d_4 at 280 K, the reaction took 14 min to reach completion.

To monitor the formation of the active complex $[Ir(H)_2(IMes)(substrate)_3]Cl$ (substrate = **4-AP** or **4-MP**), H_2 (4 bar absolute) was added to the headspace of the NMR tube. The sample was shaken vigorously for around 5 s and inserted into the NMR spectrometer (Bruker AVIII 400 MHz) at 298 K. A series of ^{1}H spectra were acquired over a period of 15.5 h (Figure S4).

Measurement of Hyperpolarized Signal. SABRE hyperpolarization transfer experiments were performed under 4 bar p-H_2 that was produced by cooling H_2 gas over a paramagnetic catalyst[8b,17] at 28 K to yield >99% *para*-enrichment. After the *para*-enriched H_2 was added to the headspace of the NMR tube, the sample was shaken for 5 s in a polarization transfer field (PTF) of 6.1 ± 0.3 mT (61 ± 3 G) generated by a hand-held magnet array,[12c] to dissolve the p-H_2 into solution and allow for polarization transfer to occur. Immediately following shaking, the sample was transferred manually into the spectrometer for a single-shot NMR measurement using either a single 90° radiofrequency (RF) pulse followed by acquisition of the FID or a variable flip angle single-shot T_1 sequence (details below). ^{1}H NMR spectra were acquired on either a Bruker AVIII 400 MHz spectrometer (9.4 T) or a Magritek Spinsolve Carbon 43 MHz benchtop NMR

DOI: 10.1021/acs.analchem.9b00729
Anal. Chem. XXXX, XXX, XXX−XXX

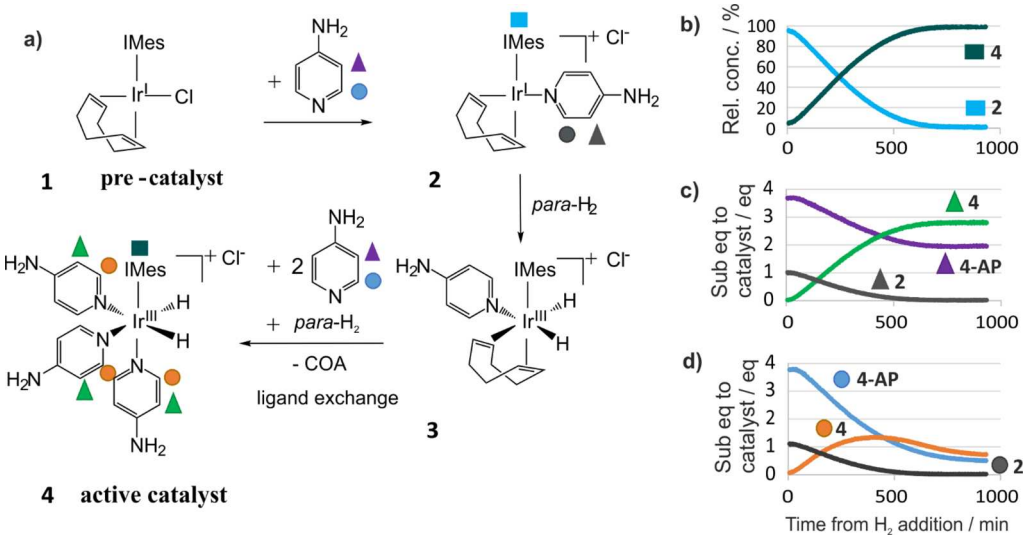

Figure 2. (a) Mechanism for the conversion of **1** to **4** in the presence of **4-AP** and H_2. First, **1** transforms into [Ir(COD)(IMes)(**4-AP**)]Cl (**2**), which then adds H_2 to form the octahedral dihydride complex [Ir(H)$_2$(COD)(IMes)(**4-AP**)]Cl (**3**), which is not stable at room temperature. COD hydrogenation then follows, and **3** converts to [Ir(H)$_2$(IMes)(**4-AP**)$_3$]Cl (**4**) by binding two more molecules of **4-AP**. (b–d) Time-dependent relative signal intensities calculated from a series of ^{1}H NMR spectra acquired over the course of the reaction at 298 K for a sample under 4 bar pressure of H_2, where the initial concentrations of **1** and **4-AP** are 5 and 25 mM, respectively. H_2 was added, and the sample was shaken only once at the start of the experiment. (b) Evolution of the carbene ligand signals of **2** (square cyan) and **4** (square teal). (c) Evolution of the *meta* proton resonance of free and bound **4-AP** (purple, gray, and green triangles). (d) Evolution of the *ortho* proton resonance of free and bound **4-AP** (blue, gray, and orange circles).

spectrometer (1 T). Between each hyperpolarization measurement, the headspace of the NMR tube was refreshed with *p*-H_2 via the diffusion between the NMR tube headspace and a line filled with fresh *p*-H_2. The sample was left to equilibrate for 10 s, and the procedure was repeated twice. This nonaggressive way of refreshing *p*-H_2 was employed to reduce solvent evaporation and thereby maintain relative catalyst and substrate concentrations throughout.

Hyperpolarized Single-Shot T_1 Measurement. The single-shot hyperpolarized T_1 measurements were achieved by acquiring a series of 15 ^{1}H NMR spectra, where the excitation pulse for each acquisition was achieved using RF pulses of increasing flip angle (see the SI for more details). The variable flip angles were chosen to excite an equal fraction of the available magnetization at each step of the experiment in order to simplify the T_1 analysis and optimize the signal-to-noise ratio. The variable time delays between acquisitions were chosen to ensure full coverage of the T_1 decay curve. To remove the influence of thermally polarized background ^{1}H NMR signals from the T_1 analysis, a reference scan was acquired after each hyperpolarized T_1 measurement. This was achieved by holding the sample outside of the NMR spectrometer for 1–1.5 min to ensure full relaxation of all polarization and then manually inserting the sample into the NMR spectrometer and carrying out a single-shot T_1 experiment. The resultant thermally polarized NMR spectra were integrated and subtracted from the hyperpolarized signals prior to T_1 analysis. Hyperpolarized relaxation times (T_1) were determined from an exponential fit of the corrected hyperpolarized signal decay according to eq 1, where $M(t)$ is magnetization, M_0 is the initial magnetization, T_1 is the time constant, t is the time since the application of the first RF pulse, and M_{offset} is the offset magnetization.

$$M(t) = M_0 e^{(-t/T_1)} + M_{offset} \quad (1)$$

Full details on the variable flip angle pulse sequence and the parameters used are available in the Supporting Information.

RESULTS

Reactivity of [Ir(COD)(IMes)(4-AP)]Cl with H_2 and 4-AP in MeOD. In order to prepare a SABRE active catalyst, a 5 mM concentration of the precatalyst with the general formula [Ir(Cl)(COD)(NHC)], where NHC is an N-heterocyclic carbene (complex **1** in Figure 2a), is mixed with an excess of the substrate. In this study, we used the substrate 4-aminopyridine (**4-AP**), a potassium channel blocker known as dalfampridine that is registered as a drug for walking improvement in patients with multiple sclerosis.[18] Once this substrate was added to the precatalyst, the chloride ion is displaced to form complex **2** (Figure 2a). When hydrogen gas was added to the resulting solution, complex **2** first oxidatively adds H_2 to form the octahedral dihydride complex **3**. The cyclooctadiene ligand in this complex was then hydrogenated to ultimately form cyclooctane (COA), which can no longer ligate. Consequently, the activated SABRE complex **4** was then formed in solution with three ligated molecules of **4-AP** and two hydrides as shown in Figure 2a.[19] When monitored by ^{1}H NMR spectroscopy at room temperature, no peaks for complex **1** were detected at 6 min (first scan). However, the transformation from **2** to **4** can be monitored through their unique NHC proton resonances at 7.32 ppm (complex **2**, cyan squares) and 6.96 ppm (complex **4**, teal squares).

This conversion can also be monitored via the *ortho* and *meta* proton resonances of **4-AP** in complex **2** (gray circles and triangles), complex **4** (orange circles and green triangles), and free solution (blue circles and purple triangles). Figure 2 presents the results of ^{1}H NMR monitoring of the SABRE catalyst activation process over a period of 15.5 h at room temperature. Figure 3 shows four representative NMR spectra obtained during the monitoring period. As illustrated in Figure

DOI: 10.1021/acs.analchem.9b00729
Anal. Chem. XXXX, XXX, XXX–XXX

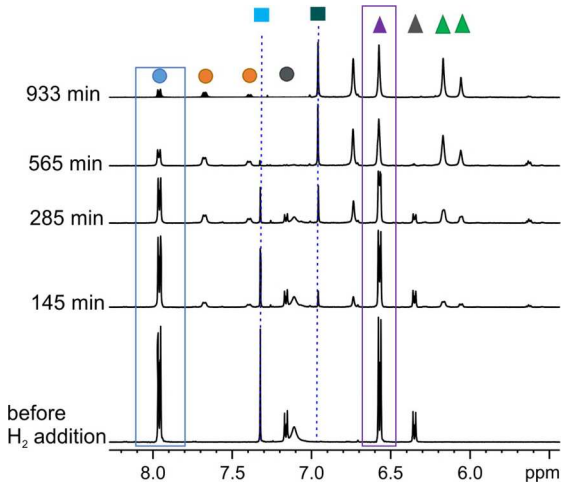

Figure 3. ^{1}H NMR spectra recorded at 9.4 T associated with the data in Figure 2 at the indicated time points with analogous color-coding to demonstrate speciation changes. It is noteworthy that the splitting on the *meta* signal for **4-AP** (6.57 ppm) evolves into a singlet because of the deuteration of the *ortho* site (7.96 ppm) over the course of the reaction. The signals of interest are surrounded by the colored boxes. The dashed lines correspond with the carbene signals in catalysts **2** and **4**.

2b, full conversion of **2** (cyan squares) to **4** (teal squares) occurs after approximately 11 h. Compared to other studies,[14b,20] the formation of **4** from **2** with **4-AP** is very slow. This is a reflection of the rate of addition of H_2 to **2**. By contrast, as described later in this paper, for the case of **4-MP**, the formation of $[Ir(H)_2(IMes)(\mathbf{4\text{-}MP})_3]Cl$ is much faster (Figure S4). This suggests that the intermediate dihydride complex forms much more rapidly when **4-MP** is the substrate. Monitoring of the *meta* resonances of **4-AP** (Figure 2c) confirms this conversion from **2** (gray triangles) to **4** (green triangles) while also demonstrating the consumption of 2 equivalents of **4-AP** in free solution (purple triangles), as expected. In contrast, the *ortho* proton resonances of **4-AP** show a different dependence on time (Figure 2d). The intensity of the *ortho* resonance of **4-AP** in complex **4** increases initially, as expected, but decays at longer times. Similarly, the intensity of the *ortho* resonance of **4-AP** in solution decays initially as expected but continues to decrease even after the formation of **4** is complete. These observations are consistent with the deuteration of the *ortho* positions of **4-AP** (Scheme 1), where the source of deuterium is the methanol-d_4, which is

Scheme 1. Deuteration of *ortho* Positions of 4-Aminopyridine in the Presence of Iridium Complexes 3 and 4 and H_2 in Methanol-d_4

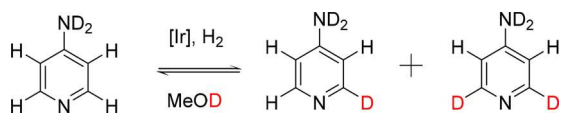

used as the solvent. These results suggest that deuteration happens on the same time scale as catalyst activation, and an analysis of the relative intensities of the *ortho* and *meta* resonances of **4-AP** indicate that the *ortho* position deuteration level reaches 75% by the end of the experiment (15.5 h). Further evidence for this *ortho* position deuteration was evident in the appearance of the corresponding ^{1}H NMR spectra, where there were significant changes in the line-shape of the *meta* resonances of **4-AP** (Figure S1). No deuteration of the *meta* positions was observed on the time scale of the experiment. Additional details and example spectra are provided in the Supporting Information.

Reaction Monitoring with SABRE. We seek to establish here that the SABRE-enhanced NMR response can be assessed through either the amplitude or the lifetime of the SABRE hyperpolarization. Both of these parameters have the potential to act as probes for reaction monitoring and require the collection of data at a series of reaction time points. The SABRE-lifetime measurements are themselves collected through a series of single-shot acquisitions that can be repeated on the time scale of five T_1 periods, which means that a typical observation time reflects a couple of minutes.[10,21] The amplitude of the SABRE signal is expected to provide information on the activation process, because the degree of signal amplification will increase as the concentration of active catalyst **4** increases. However, the effect of substrate deuteration on this signal is expected to be complicated. Previous work by Rayner et al. has suggested that deuteration can lead to increased SABRE efficiency due to a lengthening of the lifetimes of the remaining ^{1}H resonances within the substrate and the concentration of the SABRE hyperpolarization into fewer nuclei.[22] However, there is also potential for deuteration to decrease SABRE polarization transfer efficiency through changes to the *J*-coupling network that drive polarization transfer in the low-field regime.[11a,b,22,23] Observations of the changes in the SABRE-enhanced ^{1}H NMR signal intensity with time suggest that this parameter is sensitive to both of the chemical transformations under investigation (Figure S5). However, the interpretation of these effects is complicated by the fact that the SABRE response is not linearly dependent on substrate concentration in this case. In addition, any quantitative interpretation would be limited by the reproducibility of the SABRE response, which depends on many factors including *p*-H_2 enrichment level, polarization transfer field, polarization build-up time, and sample transport time. Therefore, we focus here on the use of the lifetime of the SABRE hyperpolarization to monitor reactivity.

The lifetime of the SABRE hyperpolarization is limited by longitudinal (T_1) NMR relaxation times, which are sensitive to the chemical environment and have been widely used for identifying and characterizing inter and intramolecular interactions.[24] In this method, we exploit the fact that in the presence of the active SABRE catalyst, the substrate molecules in free solution and those bound to **4** are in rapid chemical exchange. As a result, the observed lifetime of the SABRE hyperpolarization reflects a weighted average of the lifetime for substrate molecules bound to **4** and substrate molecules in free solution.[25] NMR relaxation times are known to be significantly shorter for the bound substrate molecules.[25] Therefore, as the concentration of the active SABRE catalyst **4** increases, the observed hyperpolarization lifetime is expected to decrease. This shortening of the relaxation times in the presence of the activated complex is a well-known effect in the SABRE literature.[22,25] In addition, the observed lifetime of the SABRE hyperpolarization of the *meta* resonances of **4-AP** is expected to increase following substitution of ^{2}H for ^{1}H in the adjacent *ortho* position (Scheme 1).[22,26] Therefore, the time-dependent changes of the hyperpolarization lifetimes for the *meta* resonances of **4-AP** are expected to reflect the competing effects of the formation of **4** and the partial deuteration of **4-**

DOI: 10.1021/acs.analchem.9b00729
Anal. Chem. XXXX, XXX, XXX−XXX

AP. In contrast, the hyperpolarization lifetimes for the *ortho* resonances of **4-AP** are expected to reflect only the formation of **4**. This is because a ^{1}H NMR signal will only be observed for the ^{1}H *ortho* resonances of 4-aminopyridine and 4-amino-2-d_1-pyridine. In both of these cases, the observed *ortho* ^{1}H hyperpolarization lifetime will be dominated by interactions with the ^{1}H in the adjacent *meta* position and therefore is not expected to be affected significantly by the progress of the ^{1}H−^{2}H exchange reaction.[22]

Parallel measurements of non-hyperpolarized ^{1}H NMR spectra and hyperpolarization lifetimes were performed as a function of time following the first addition of *p*-H_2 with detection on a 400 MHz NMR spectrometer in methanol-d_4 (Figure 4a and b). Non-hyperpolarized ^{1}H NMR spectra

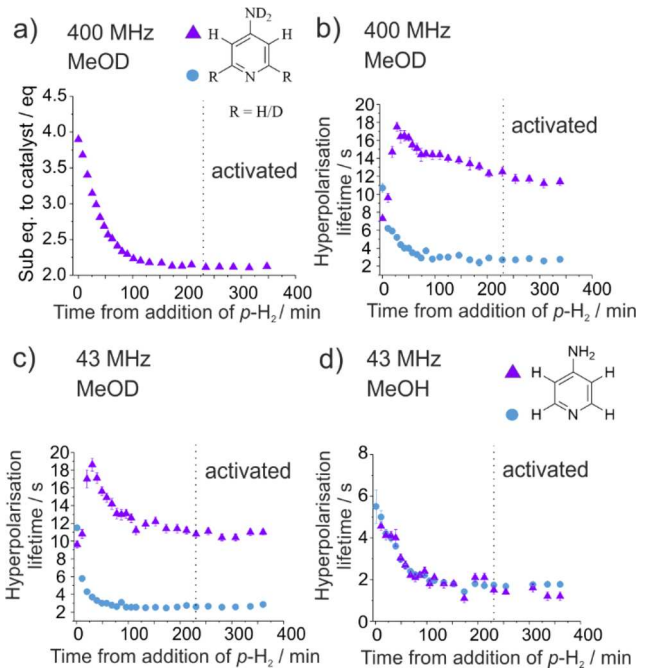

Figure 4. (a) Non-hyperpolarized ^{1}H NMR signal integrals of the **4-AP** *meta* proton resonance, acquired in parallel with the hyperpolarization-lifetime measurements (b) at 400 MHz in methanol-d_4. (b) Hyperpolarization signal lifetimes of the *ortho* (blue circles) and *meta* (purple triangles) proton resonances of **4-AP** as a function of time after H_2 addition in methanol-d_4 at 9.4 T, (c) as (b) but recorded at 1 T and (d) as (c) but in *protio* methanol. The initial concentration of **4-AP** is 25 mM, which gives a 2-fold excess relative to $[Ir(H)_2(IMes)(\mathbf{4\text{-}AP})_3]Cl$ (5 mM) once its formation is complete. Error bars indicate the standard error from the fit to the hyperpolarization decay curve specified by eq 1. The time point for complete conversion to **4** is represented by the vertical line.

indicate that the formation of **4** is complete by 230 min following the first addition of *p*-H_2 (Figure 4a). This activation time is indicated by the vertical dashed lines in Figure 4b−d. Figure 4b shows the change in the *ortho* (blue circles) and *meta* (purple triangles) ^{1}H hyperpolarization lifetimes as a function of time following the initial addition of *p*-H_2. Each hyperpolarization-lifetime measurement is achieved using a manual shaking SABRE procedure with NMR detection at 9.4 T and where the *p*-H_2 in the headspace of the NMR tube was refreshed between each measurement. In Figure 4b, the hyperpolarization lifetimes for the *ortho* resonances of **4-AP** reduce and reach a plateau in a time period that corresponds to the formation of **4**. In contrast, the lifetimes of the *meta* resonances show an initial rapid increase with a subsequent decrease at longer times. These observations support our hypothesis that the hyperpolarization lifetimes of the *meta* resonances are sensitive to both the formation of **4** and substrate deuteration, whereas the hyperpolarization lifetimes of the *ortho* resonances are sensitive only to the formation of **4**. The initial change in the lifetime of the *meta* resonances indicates a more rapid incorporation of ^{2}H into **4-AP** when *p*-H_2 was replenished between measurements rather than added once at the start of the experiment (Figure 2). This increase in the rate of the HIE reaction is supported by the observed changes in the line shape of the *meta* resonances in the standard ^{1}H NMR spectra acquired at 400 MHz (Figure S3).

The use of SABRE hyperpolarization to increase sensitivity allows us to repeat this reaction monitoring procedure on a 1 T benchtop NMR spectrometer (Figure 4c). The time-dependent changes in hyperpolarization lifetime determined using the benchtop NMR instrument show the same trends as the experiments using a standard (9.4 T) NMR spectrometer. This illustrates that SABRE hyperpolarization can be used to enable reaction monitoring at both high- and low-field. In fact, here we use benchtop NMR where a combination of low sensitivity and peak overlap would normally prevent this monitoring process. Furthermore, once the sensitivity limitation is overcome through the use of hyperpolarization, there are additional benefits to using benchtop NMR. Because of its lower magnetic field strength, benchtop ^{1}H NMR spectra can be acquired in the presence of a protonated solvent without the need to actively suppress the solvent signal. Indeed, it has been found that the SABRE-hyperpolarized NMR response from a low-concentration analyte can exceed that from a protonated solvent when detected at 1 T (43 MHz).[12b] Figure 4d shows the change in the *ortho* (blue circles) and *meta* (purple triangles) ^{1}H hyperpolarization lifetimes as a function of time following the initial addition of *p*-H_2 for the case where *protio* methanol is the solvent and a 1 T benchtop NMR spectrometer are used for detection. In the absence of the source of deuterium (methanol-d_4) the hyperpolarization lifetimes of both the *ortho* and *meta* protons follow the same trend: a monotonic decrease to a plateau on the same time scale as the formation of the activated SABRE complex, **4**. The absence of the initial increase in the *meta* hyperpolarization lifetime supports the hypothesis that this feature of the previous experiments originated from the deuteration effect. Therefore, not only does the use of SABRE hyperpolarization enable reaction monitoring using a benchtop NMR spectrometer, but also the use of this low-field (1 T) instrument provides a simple route to the deconvolution of the competing effects of SABRE catalyst activation and substrate deuteration.

To further verify the method, we have applied it to an analogous SABRE system where the substrate is 4-methylpyridine (**4-MP**). When the reaction is monitored after a single exposure to H_2, even though rapid formation of $[Ir(H)_2(IMes)(\mathbf{4\text{-}MP})_3]Cl$ (~50 min) is indicated, the time scale for deuteration is comparable to that with **4-AP**. This suggests that $[Ir(H)_2(IMes)(\mathbf{4\text{-}AP})_3]Cl$ is more active for the HIE reaction than $[Ir(H)_2(IMes)(\mathbf{4\text{-}MP})_3]Cl$ (Figure S4). This difference in behavior is consistent with the predicted C−H bond strengths in the substrates on the basis of inductive changes. One further consequence of this behavior is that when the hyperpolarized lifetimes are probed over the first 65 min, rapid catalyst activation is observed with negligible

DOI: 10.1021/acs.analchem.9b00729
Anal. Chem. XXXX, XXX, XXX−XXX

deuteration. The analogous hyperpolarized lifetimes in protonated methanol exhibit the same trend, further supporting the deduction of the absence of significant deuteration on the time scale of the experiment (Figures S9 and S10).

CONCLUSIONS

We have introduced a method for using SABRE-enhanced ^{1}H NMR spectroscopy to monitor reactivity, even at a mM concentration level, through the quantification of hyperpolarization lifetimes. This method was used to monitor the formation of the active SABRE catalyst from a precatalyst and hydrogen isotope exchange within the substrate, 4-aminopyridine. This method was demonstrated using both high-field (9.4 T, 400 MHz) and benchtop (1 T, 43 MHz) NMR detection. Comparable results were obtained at both fields, illustrating the utility of this approach for reaction monitoring on a benchtop NMR spectrometer even under conditions where thermal ^{1}H NMR cannot be used due to low sensitivity and peak overlap. In addition, the use of a low-field benchtop NMR spectrometer for detection allowed experiments to be carried out in a *protio* solvent. For the reactivity explored herein, this provided a route to separating out the effects of the formation of the SABRE catalyst and the hydrogen isotope exchange reaction, by removing the source of ^{2}H for the isotope exchange, methanol-d_4. More generally, the ability to carry out reaction monitoring in a nondeuterated solvent renders this method more attractive for industrial applications where metal complexes are used to achieve high-value organic transformations, as it removes the need for costly sample preparation step prior to analysis.[27]

The studies completed in this work followed reactivity under two different regimes within a sealed NMR tube: first, in the absence of stirring where slow diffusion of hydrogen across the gas−liquid interface is expected and second, where hydrogen in solution was replenished between experiments through vigorous shaking of the NMR tube. In future work, a flow-based SABRE approach, where p-H_2 is bubbled through the solution outside of the spectrometer,[28] could provide a route to automating the reaction monitoring method and providing more control over the reaction conditions.

In situ SABRE measurements, where detection is achieved in mT−μT magnetic fields such as the Earth's magnetic field, could also be used to provide increased control over the reaction conditions throughout the monitoring process. However, in this case, there would be a need for reference measurements to isolate the source of the hyperpolarized response, as no chemical shift information is available in such ultralow-field NMR spectra. The quantitative aspects of the method can be improved by calibrating the hyperpolarization lifetimes to link changes in lifetime to changes in the concentration of the active SABRE species.

ASSOCIATED CONTENT

Supporting Information

The Supporting Information is available free of charge on the ACS Publications website at DOI: 10.1021/acs.analchem.9b00729.

Quantification of substrate to catalyst ratios and the level of deuterium incorporation; evidence of the 4-aminopyridine (**4-AP**) *ortho* position deuteration; standard ^{1}H NMR reaction monitoring of the SABRE catalyst activation with 4-aminopyridine (**4-AP**) and 4-methylpyridine (**4-MP**); reaction monitoring with SABRE signal; variable flip angle single-shot sequence for relaxation time measurements; activation monitoring with 4-methylpyridine using hyperpolarization lifetimes; characterization (PDF)

AUTHOR INFORMATION

Corresponding Authors

*E-mail: meghan.halse@york.ac.uk. (M.E.H.)
*E-mail: simon.duckett@york.ac.uk. (S.B.D.)

ORCID

Peter M. Richardson: 0000-0002-6631-2459
Simon B. Duckett: 0000-0002-9788-6615

Notes

The authors declare no competing financial interest.
NMR data can be found at: https://doi.org/10.15124/723cd7c0-dbeb-4ad1-9e5d-93639db9b38c.

ACKNOWLEDGMENTS

The authors would like to thank Dr. Richard John for NMR support, Dr. Victoria Annis for synthesis of the SABRE catalyst, and the EPSRC (EP/M020983/1) and Wellcome Trust (092506 and 098335) for funding. O.S. would like to thank Pfizer, the Department of Chemistry Wild Fund Scholarship, and the University of York for Ph.D. studentship funding.

REFERENCES

(1) (a) Bakeev, K. A. In *Process analytical technology: spectroscopic tools and implementation strategies for the chemical and pharmaceutical industries*, 1st ed.; Bakeev, K. A., Ed.; Blackwell Publishing Ltd: Oxford, UK, 2005; pp 13−39. (b) Rathore, A. S.; Bhambure, R.; Ghare, V. *Anal. Bioanal. Chem.* **2010**, *398* (1), 137−154.

(2) (a) Sans, V.; Porwol, L.; Dragone, V.; Cronin, L. *Chem. Sci.* **2015**, *6* (2), 1258−1264. (b) Musio, B.; Gala, E.; Ley, S. V. *ACS Sustainable Chem. Eng.* **2018**, *6* (1), 1489−1495. (c) Singh, K.; Danieli, E.; Blümich, B. *Anal. Bioanal. Chem.* **2017**, *409* (30), 7223−7234. (d) Schumacher, S. U.; Rothenhäusler, B.; Willmann, A.; Thun, J.; Moog, R.; Kuentz, M. *J. Pharm. Biomed. Anal.* **2017**, *137*, 96−103. (e) Blümich, B. *TrAC, Trends Anal. Chem.* **2016**, *83*, 2−11. (f) Meyer, K.; Kern, S.; Zientek, N.; Guthausen, G.; Maiwald, M. *TrAC, Trends Anal. Chem.* **2016**, *83*, 39−52. (g) Singh, K.; Blümich, B. *TrAC, Trends Anal. Chem.* **2016**, *83*, 12−26.

(3) (a) Halse, M. E. *TrAC, Trends Anal. Chem.* **2016**, *83*, 76−83. (b) Ardenkjaer-Larsen, J. H.; Boebinger, G. S.; Comment, A.; Duckett, S.; Edison, A. S.; Engelke, F.; Griesinger, C.; Griffin, R. G.; Hilty, C.; Maeda, H.; Parigi, G.; Prisner, T.; Ravera, E.; van Bentum, J.; Vega, S.; Webb, A.; Luchinat, C.; Schwalbe, H.; Frydman, L. *Angew. Chem., Int. Ed.* **2015**, *54* (32), 9162−9185.

(4) Ardenkjaer-Larsen, J. H. *J. Magn. Reson.* **2016**, *264*, 3−12.

(5) (a) Berthault, P.; Huber, G.; Desvaux, H. *Prog. Nucl. Magn. Reson. Spectrosc.* **2009**, *55* (1), 35−60. (b) Walker, T. G.; Happer, W. *Rev. Mod. Phys.* **1997**, *69* (2), 629−642.

(6) (a) Duckett, S. B.; Mewis, R. E. *Acc. Chem. Res.* **2012**, *45* (8), 1247−1257. (b) Hovener, J.; Pravdivtsev, A. N.; Kidd, B.; Bowers, C. R.; Glöggler, S.; Kovtunov, K. V.; Plaumann, M.; Katz-Brull, R.; Buckenmaier, K.; Jerschow, A.; Reineri, F.; Theis, T.; Shchepin, R. V.; Wagner, S.; Zacharias, N. M.; Bhattacharya, P.; Chekmenev, E. Y. *Angew. Chem., Int. Ed.* **2018**, *57*, 11140.

(7) (a) Tee, S. S.; DiGialleonardo, V.; Eskandari, R.; Jeong, S.; Granlund, K. L.; Miloushev, V.; Poot, A. J.; Truong, S.; Alvarez, J. A.; Aldeborgh, H. N.; Keshari, K. R. *Sci. Rep.* **2016**, *6*, 32846. (b) Hirsch, M. L.; Kalechofsky, N.; Belzer, A.; Rosay, M.; Kempf, J. G. *J. Am. Chem. Soc.* **2015**, *137* (26), 8428−8434.

DOI: 10.1021/acs.analchem.9b00729
Anal. Chem. XXXX, XXX, XXX−XXX

(8) (a) Duckett, S. B.; Sleigh, C. J. *Prog. Nucl. Magn. Reson. Spectrosc.* **1999**, *34* (1), 71−92. (b) Natterer, J.; Bargon, J. *Prog. Nucl. Magn. Reson. Spectrosc.* **1997**, *31* (4), 293−315.
(9) Bowers, C. R.; Weitekamp, D. P. *Phys. Rev. Lett.* **1986**, *57* (21), 2645−2648.
(10) Adams, R. W.; Aguilar, J. A.; Atkinson, K. D.; Cowley, M. J.; Elliott, P. I. P.; Duckett, S. B.; Green, G. G. R.; Khazal, I. G.; López-Serrano, J.; Williamson, D. C. *Science* **2009**, *323* (5922), 1708.
(11) (a) Theis, T.; Truong, M. L.; Coffey, A. M.; Shchepin, R. V.; Waddell, K. W.; Shi, F.; Goodson, B. M.; Warren, W. S.; Chekmenev, E. Y. *J. Am. Chem. Soc.* **2015**, *137* (4), 1404−1407. (b) Ivanov, K. L.; Pravdivtsev, A. N.; Yurkovskaya, A. V.; Vieth, H.-M.; Kaptein, R. *Prog. Nucl. Magn. Reson. Spectrosc.* **2014**, *81*, 1−36. (c) Adams, R. W.; Duckett, S. B.; Green, R. A.; Williamson, D. C.; Green, G. G. R. *J. Chem. Phys.* **2009**, *131* (19), 194505.
(12) (a) Colell, J. F. P.; Emondts, M.; Logan, A. W. J.; Shen, K.; Bae, J.; Shchepin, R. V.; Ortiz, G. X.; Spannring, P.; Wang, Q.; Malcolmson, S. J.; Chekmenev, E. Y.; Feiters, M. C.; Rutjes, F. P. J. T.; Blümich, B.; Theis, T.; Warren, W. S. *J. Am. Chem. Soc.* **2017**, *139* (23), 7761−7767. (b) Richardson, P. M.; Parrott, A. J.; Semenova, O.; Nordon, A.; Duckett, S. B.; Halse, M. E. *Analyst* **2018**, *143* (14), 3442−3450. (c) Richardson, P. M.; Jackson, S.; Parrott, A. J.; Nordon, A.; Duckett, S. B.; Halse, M. E. *Magn. Reson. Chem.* **2018**, *56* (7), 641−650. (d) Lehmkuhl, S.; Wiese, M.; Schubert, L.; Held, M.; Küppers, M.; Wessling, M.; Blümich, B. *J. Magn. Reson.* **2018**, *291*, 8−13.
(13) (a) Iali, W.; Rayner, P. J.; Duckett, S. B. *Science Advances* **2018**, *4* (1), eaao6250. (b) Logan, A. W. J.; Theis, T.; Colell, J. F. P.; Warren, W. S.; Malcolmson, S. J. *Chem. - Eur. J.* **2016**, *22* (31), 10777−10781. (c) Zeng, H.; Xu, J.; Gillen, J.; McMahon, M. T.; Artemov, D.; Tyburn, J.-M.; Lohman, J. A. B.; Mewis, R. E.; Atkinson, K. D.; Green, G. G. R.; Duckett, S. B.; van Zijl, P. C. M. *J. Magn. Reson.* **2013**, *237*, 73−78. (d) Shchepin, R. V.; Jaigirdar, L.; Chekmenev, E. Y. *J. Phys. Chem. C* **2018**, *122* (9), 4984−4996.
(14) (a) Manoharan, A.; Rayner, P. J.; Fekete, M.; Iali, W.; Norcott, P.; Hugh Perry, V.; Duckett, S. B. *ChemPhysChem* **2019**, *20* (2), 285−294. (b) Shi, F.; Coffey, A. M.; Waddell, K. W.; Chekmenev, E. Y.; Goodson, B. M. *J. Phys. Chem. C* **2015**, *119* (13), 7525−7533. (c) Nelson, S. J.; Kurhanewicz, J.; Vigneron, D. B.; Larson, P. E. Z.; Harzstark, A. L.; Ferrone, M.; van Criekinge, M.; Chang, J. W.; Bok, R.; Park, I.; Reed, G.; Carvajal, L.; Small, E. J.; Munster, P.; Weinberg, V. K.; Ardenkjaer-Larsen, J. H.; Chen, A. P.; Hurd, R. E.; Odegardstuen, L.-I.; Robb, F. J.; Tropp, J.; Murray, J. A. *Sci. Transl. Med.* **2013**, *5* (198), 198ra108. (d) Tickner, B. J.; Iali, W.; Roy, S. S.; Whitwood, A. C.; Duckett, S. B. *ChemPhysChem* **2019**, *20* (2), 241−245.
(15) Appleby, K. M.; Mewis, R. E.; Olaru, A. M.; Green, G. G. R.; Fairlamb, I. J. S.; Duckett, S. B. *Chem. Sci.* **2015**, *6* (7), 3981−3993.
(16) (a) Eshuis, N.; Hermkens, N.; van Weerdenburg, B. J. A.; Feiters, M. C.; Rutjes, F. P. J. T.; Wijmenga, S. S.; Tessari, M. *J. Am. Chem. Soc.* **2014**, *136* (7), 2695−2698. (b) Fekete, M.; Bayfield, O.; Duckett, S. B.; Hart, S.; Mewis, R. E.; Pridmore, N.; Rayner, P. J.; Whitwood, A. *Inorg. Chem.* **2013**, *52* (23), 13453−13461. (c) van Weerdenburg, B. J. A.; Gloggler, S.; Eshuis, N.; Engwerda, A. H. J.; Smits, J. M. M.; de Gelder, R.; Appelt, S.; Wymenga, S. S.; Tessari, M.; Feiters, M. C.; Blumich, B.; Rutjes, F. P. J. T. *Chem. Commun.* **2013**, *49* (67), 7388−7390. (d) Ellames, G. J.; Gibson, J. S.; Herbert, J. M.; McNeill, A. H. *Tetrahedron* **2001**, *57* (46), 9487−9497. (e) Barskiy, D. A.; Kovtunov, K. V.; Koptyug, I. V.; He, P.; Groome, K. A.; Best, Q. A.; Shi, F.; Goodson, B. M.; Shchepin, R. V.; Coffey, A. M.; Waddell, K. W.; Chekmenev, E. Y. *J. Am. Chem. Soc.* **2014**, *136* (9), 3322−3325.
(17) Tom, B. A.; Bhasker, S.; Miyamoto, Y.; Momose, T.; McCall, B. J. *Rev. Sci. Instrum.* **2009**, *80* (1), No. 016108.
(18) Blight, A. R. *Ther. Adv. Neurol. Disord.* **2011**, *4* (2), 99−109.
(19) Crabtree, R. *Acc. Chem. Res.* **1979**, *12* (9), 331−337.
(20) (a) Truong, M. L.; Shi, F.; He, P.; Yuan, B.; Plunkett, K. N.; Coffey, A. M.; Shchepin, R. V.; Barskiy, D. A.; Kovtunov, K. V.; Koptyug, I. V.; Waddell, K. W.; Goodson, B. M.; Chekmenev, E. Y. *J. Phys. Chem. B* **2014**, *118* (48), 13882−13889. (b) Cowley, M. J.; Adams, R. W.; Atkinson, K. D.; Cockett, M. C. R.; Duckett, S. B.; Green, G. G. R.; Lohman, J. A. B.; Kerssebaum, R.; Kilgour, D.; Mewis, R. E. *J. Am. Chem. Soc.* **2011**, *133* (16), 6134−6137.
(21) (a) Golman, K.; Ardenkjær-Larsen, J. H.; Petersson, J. S.; Månsson, S.; Leunbach, I. *Proc. Natl. Acad. Sci. U. S. A.* **2003**, *100* (18), 10435. (b) Kaptein, R.; Dijkstra, K.; Tarr, C. E. *J. Magn. Reson.* **1976**, *24* (2), 295−300.
(22) Rayner, P. J.; Burns, M. J.; Olaru, A. M.; Norcott, P.; Fekete, M.; Green, G. G. R.; Highton, L. A. R.; Mewis, R. E.; Duckett, S. B. *Proc. Natl. Acad. Sci. U. S. A.* **2017**, *114* (16), E3188−E3194.
(23) (a) Green, R. A.; Adams, R. W.; Duckett, S. B.; Mewis, R. E.; Williamson, D. C.; Green, G. G. R. *Prog. Nucl. Magn. Reson. Spectrosc.* **2012**, *67*, 1−48. (b) Eshuis, N.; Aspers, R. L. E. G.; van Weerdenburg, B. J. A.; Feiters, M. C.; Rutjes, F. P. J. T.; Wijmenga, S. S.; Tessari, M. *J. Magn. Reson.* **2016**, *265*, 59−66.
(24) (a) Kumar, D.; Krishnan, Y.; Paranjothy, M.; Pal, S. *J. Phys. Chem. B* **2017**, *121* (13), 2864−2872. (b) Kim, J.; Liu, M.; Hilty, C. *J. Phys. Chem. B* **2017**, *121* (27), 6492−6498. (c) Fairhurst, D.; Cosgrove, T.; Prescott, S. W. *Magn. Reson. Chem.* **2016**, *54* (6), 521−526. (d) Grant, D. M.; Mayne, C. L.; Liu, F.; Xiang, T. X. *Chem. Rev. (Washington, DC, U. S.)* **1991**, *91* (7), 1591−1624.
(25) Mewis, R. E.; Fekete, M.; Green, G. G. R.; Whitwood, A. C.; Duckett, S. B. *Chem. Commun.* **2015**, *51* (48), 9857−9859.
(26) Taglang, C.; Korenchan, D. E.; von Morze, C.; Yu, J.; Najac, C.; Wang, S.; Blecha, J. E.; Subramaniam, S.; Bok, R.; VanBrocklin, H. F.; Vigneron, D. B.; Ronen, S. M.; Sriram, R.; Kurhanewicz, J.; Wilson, D. M.; Flavell, R. R. *Chem. Commun.* **2018**, *54* (41), 5233−5236.
(27) (a) Busacca, C. A.; Fandrick, D. R.; Song, J. J.; Senanayake, C. H. *Adv. Synth. Catal.* **2011**, *353* (11−12), 1825−1864. (b) Thompson, D. T. *Coord. Chem. Rev.* **1996**, *154*, 179−192.
(28) Hovener, J. B.; Schwaderlapp, N.; Borowiak, R.; Lickert, T.; Duckett, S. B.; Mewis, R. E.; Adams, R. W.; Burns, M. J.; Highton, L. A. R.; Green, G. G. R.; Olaru, A.; Hennig, J.; von Elverfeldt, D. *Anal. Chem.* **2014**, *86* (3), 1767−1774.

DOI: 10.1021/acs.analchem.9b00729
Anal. Chem. XXXX, XXX, XXX−XXX